Food Research International 44 (2011) 2938–2948

Contents lists available at ScienceDirect

Food Research International

journal homepage: www.elsevier.com/locate/foodres

Structure (micro, ultra, nano), color and mechanical properties of *Vitis labrusca* L. (grape berry) fruits treated by hydrogen peroxide, UV–C irradiation and ultrasound

Joaquín Fava [a,1], Karina Hodara [c], Andrea Nieto [b,2], Sandra Guerrero [b,2], Stella Maris Alzamora [b,2], María Agueda Castro [a,*]

[a] Anatomía Vegetal Aplicada, Departamento de Biodiversidad y Biología Experimental, Universidad de Buenos Aires, Ciudad Universitaria, 1428 C.A.B.A., Argentina
[b] Departamento de Industrias, Facultad de Ciencias Exactas y Naturales, Universidad de Buenos Aires, Ciudad Universitaria, 1428 C.A.B.A., Argentina
[c] Departamento de Métodos Cuantitativos y Sistemas de Información, Facultad de Agronomía, Universidad de Buenos Aires, Av. San Martín 4453, C1417DSE C.A.BA., Argentina

ARTICLE INFO

Article history:
Received 4 April 2011
Accepted 30 June 2011

Keywords:
Grape berry
Structure
Mechanical properties
Color
UV–C
Hydrogen peroxide
Ultrasound

ABSTRACT

Main structural (micro, ultra, and nano) alterations occurred in the outer tangential epidermal cell wall of *Vitis labrusca* L. fruits (grape berry) due to hydrogen peroxide, UV–C irradiation and ultrasound treatments were examined, and described using light microscopy, scanning electron microscopy, transmission electron microscopy and atomic force microscopy. Changes in mechanical properties and surface color were also evaluated. In general, decontamination treatments caused epicuticular wax pattern alteration, epicarp disruptions, cell plasmolysis, and mesocarp collapse. Major observed ultrastructural and nanostructural changes were increased demarcation between cellulose layer and cuticular membrane, alteration of cellulose aggregates pattern, and presence of nanofractures, variables in shape and size. All treatments, mainly ultrasound, provoked significant but small differences in color parameters compared to untreated fruit. On contrast, mechanical properties determined by puncture test did not vary.

© 2011 Elsevier Ltd. All rights reserved.

1. Introduction

High quality fruits are now strongly demanded by consumers, interested in their role for maintaining and improving human well-being (Allende, Tomás-Barberán, & Gil, 2006). Grape berries have become increasingly popular not only because of their direct implication in wine industry and related viticulture activities, but also their phenol content and antioxidant activity (González-Paramás, Esteban-Ruano, Santos-Buelga, de Pascual-Teresa, & Rivas-Gonzalo, 2004).

Microorganisms are natural contaminants of fresh produce. Sanitation of whole fruit is conducted generally with an initial washing in tap water to eliminate pesticide residues, dirt and plant debris, followed by a dip in sodium hypochlorite containing water to effectively reduce the microbial load on the fruit surface. Then sanitized fruits are usually preserved by cooling or by modified atmosphere storage. However, alternative decontamination methods (for instance hydrogen peroxide, UV–C irradiation, ozone or high power ultrasound treatments) have been proposed because of the association of chlorine with the formation of carcinogenic chlorinated compounds and its low effectiveness in reducing microorganism population in surface of fruits (Beuchat, 2000).

The quality of fruits is based on several attributes: flavor, texture, color, and nutritional and functional characteristics. It is known that dynamic changes in cell wall chemical composition as well as in the tissue structure during ripening, senescence, storage, post harvest and processing cause some variations in grape sensory, chemical and physical properties (Carreño, Martínez, Almela, & Fernández-López, 1995). However, little is known about micro and ultrastructural effects of alternative decontamination techniques as well as their impact on grape quality.

The skin represents about 5–10% of the total dry weight of grape berry, and acts as a hydrophobic barrier to protect the fruit from physiological and climatic injuries, dehydration, fungal infection, and UV–C light (Pinelo, Arnous, & Meyer, 2006). Epidermal cell wall can be distinguished from all other cell walls of plants by the presence of thick continuous lipidic layers (cuticular membrane) deposited on its outermost region (Jeffree, Baker, & Holloway, 1976; Wattendorff & Holloway, 1980). In general, five defined layers have been described from outer to inner: 1. epicuticular wax layer (amorphous, crystalline or semi-crystalline); 2. cuticle proper (constituted only by cutin); 3. cutinized layer (mainly composed by a polysaccharide matrix, cutin, and intracuticular waxes). The cuticle proper and the cutinized layer constitute the cuticular membrane (Esau,1977); 4. pectic layer (mainly composed by pectic polysaccharides), and 5. non cutinized

* Corresponding author. Tel.: +54 11 45763300 (385).
E-mail addresses: alzamora@di.fcen.uba.ar (S.M. Alzamora), mac@bg.fcen.uba.ar (M.A. Castro).
[1] Fellowship of Consejo National de Investigaciones Científicas y Técnicas de la República Argentina, Argentina.
[2] Member of Consejo Nacional de Investigaciones Científicas y Técnicas de la República Argentina, Argentina.

0963-9969/$ – see front matter © 2011 Elsevier Ltd. All rights reserved.
doi:10.1016/j.foodres.2011.06.053

cellulose layer or cellulose layer (Baker, 1982; Holloway, 1982), which is a strong network of cellulose microfibrils linked by hydrogen bonding to xyloglucans, pectic polysaccharides, and additional minor cell wall constituents (structural proteins, enzymatic proteins, hydrophobic compounds and inorganic molecules) (Carpita & Gibeaut, 1993; Cosgrove, 2001). Next to epidermis, hypodermis with abundant phenolic compounds appears constituted by several (3–4) cell layers (González-Paramás et al., 2004).

In particular, Radler and Horn (1965) found the presence of both hard wax, mainly of oleanolic acid, and soft wax of alcohols, aldehydes, esters, fatty acids, hydrocarbons, and oleanolic acids in the epicuticular wax layer of *V. labrusca* L. Rosenquist and Morrison (1988) reported in *V. vinifera* L. mature grapes the presence of epicuticular waxes like platelets. Casado and Heredia (2001) concluded that the cuticular material performed at maturity a smooth, continuous and homogeneous cuticle about 3 μm thick.

There is scarce information in the literature on mechanical analysis of grape berries. Most of the scientific contributions were mainly concerned with the study of mechanical properties evolution during ripening, Huang, Huang, and Wang (2005) analyzed, prior and after ripeness, the mechanical properties and cell wall changes of grape skin from cv. Golden Muscat (*V. vinifera* L. × *V. labrusca* L.). The authors concluded that, after ripeness, skin strength and elasticity dropped severely, and the loss of cell wall polysaccharides was compensated by the inclusion of structural proteins. Letaief, Rolle, Zeppa, and Gerbi (2006) focused their interest on grape texture measurement as a grape maturity index, and reported not significant differences between berries picked from different bunch positions.

In relation to color, anthocyanins are mainly present in the grape skin. Therefore, external grape color and anthocyanic profile are closely linked. Fernández-López, Almela, Muñoz, Hidalgo, and Carreño (1999) provided information about anthocyanin accumulation in grapes during ripening, and analyzed the dependence between color and individual anthocyanin content. Based on the C.I.E. $L^*a^*b^*$ (CIELAB) color space specified by the Commission Internationale de l'Eclairage, Carreño et al. (1995) described a new color index to distinguish between grape groups of different external color.

The present study was aimed to: examine the main structural alterations occurred in the outer tangential epidermal cell wall, and analyze the changes in surface color and mechanical properties of *Vitis labrusca* L. (grape berry) fruits caused by hydrogen peroxide, UV–C irradiation and high power ultrasound treatments. Structural, mechanical and color analyses of raw and treated grapes would help to identify alterations caused by treatments providing new insights to optimize disinfection processes.

2. Materials and methods

2.1. Sample preparation

Grapes (*V. labrusca* L.), cv. Isabella, were harvested from plants growing in Palo Blanco vineyard, Berisso, Buenos Aires province, Argentina. Bunches of raw grape berries (about 15–20 mm in diameter, 18.0 ± 0.2 °Brix) were randomly picked with attached pedicels. Then, they were placed in polyethylene bags and maintained at 4–5 °C for a maximum time of 2 days before use.

Four groups of 45 grape berry fruits with similar shape and color, and without detaching the pedicel, were randomly taken from different positions of the bunch. Samples were subjected to different treatments: one group to UV–C radiation, one to hydrogen peroxide immersion and one to high power ultrasound. Another group of raw fruits was selected as control. The treated and raw groups were examined for structure, color and mechanical properties immediately after treatments.

2.2. Hydrogen peroxide treatment

Treatment was carried out at 25 °C in a 900 ml glass flask with 600 ml of sterile citric acid–Na_2HPO_4 buffer solution (pH 3.0) containing 34.3 mL of hydrogen peroxide to obtain a final solution with 2.0% (w/v) concentration. The disinfectant agent solution was prepared from 35% (w/v) hydrogen peroxide solution (Merck, Darmstadt, Germany). The buffer solution was prepared from 0.1 M citric acid monohydrate (J.T. Baker, Phillipsburg, USA) and 0.2 M Na_2HPO_4 (M&B, Dagenham, England). H_2O_2 levels were monitored by titration with 0.1 N potassium permanganate (Mallinckrodt, Phillipsburg, USA) immediately before and after treatment. The pH was measured with a pH meter METTLER TOLEDO (model MP 220, Schwerzenbach, Switzerland).

Buffer solution was prepared with deionized water obtained from a Milli-Q system (Model OM-140, Millipore, Billerica, USA). The solution was prepared 15 min before be used. Berries were immersed during 2 min in the sanitizing agent solution, and then were transferred into a bath of distilled water at 25 °C as neutralizing solution by 1 min.

Sanitizing conditions (pH, hydrogen peroxide concentration and immersion time) were selected due to their great effectiveness against microorganisms, according to previous studies reported by Raffellini, Guerrero, and Alzamora (2008).

2.3. UV–C treatment

The UV–C irradiation device consisted of one bank of two reflectors with unfiltered germicidal emitting lamps (253.7 nm, TUV-15 W G13 T8 55 V, Philips, Holland) located 10 cm above the produce tray. The UV–C lamps and the treatment area were enclosed in a wooden box covered with aluminum foil with a cover protection for the operators. A ventilation device was placed in a corner of the box to avoid temperature increase due to UV–C radiation. The mean temperature during the treatments was 27 ± 1 °C. Prior to use, the UV–C lamps were allowed to stabilize by turning them on at least 15 min.

The UV–C intensities emitted from the lamps were determined using the iodide/iodate chemical actinometer (Rahn, 1997). All reactives employed in UV–C dosimetry were analytical grade from Merck Química Argentina S.A. (Argentina). Variations in radiation dose absorption were minimized by placing the samples within a uniform area of the radiation field (between the lamps and equidistant with respect to lamp streams).

Grape berry samples were placed on the tray forming a single layer and exposed on one side to irradiation for 15 min. The UV–C dose received after this treatment was 8.4 ± 0.5 kJ/m^2. Irradiated grape berries were compared with untreated grape berries (raw fruits) held 15 min at a temperature (~27 ± 1 °C) similar to that of treated berries during irradiation but without being exposed to UV–C light. The UV–C radiation level was selected according to literature studies conducted in similar conditions for the inactivation of microorganisms on the surface of many fruits (Gardner & Shama, 2000; Marquenie et al., 2002; Nigro, Hipólito, & Lima, 1998).

2.4. Ultrasonic treatment

Treatment was carried out in a 500 mL-double wall cylindrical vessel (diameter: 9.5 cm; height: 14.5 cm) connected to a thermostatically controlled water bath (HAAKE, Model Rotovisco RV12, Germany) whose temperature was fixed to attain 30 °C in the samples. Eight fruits were placed in a fixed stainless steel net into the vessel at 15 mm of distance between tip and samples, around the 13 mm ultrasound probe (tip size: 12.7 mm) and 400 mL distilled water was added. The fruits were immediately sonicated.

Ultrasound (Vibracell®, net power output: 600 W, Sonic Materials Inc., Chicago) at 20 kHz and 95.2 (80%) μm of wave amplitude was applied to the grape berries during 5 min. Ultrasound times greater than 5 min provoked rupture of grape skin. After 2 or 3 min of sonication, the desired temperature was reached and it was maintained constant throughout the experiment by recycling water 10 °C below the selected value. Due to bubbles generated by cavitation, the system was always highly mixed from the start of the experiment.

Previous studies have shown that the selected amplitude of ultrasonic process was the most suitable, since further increases in amplitude did not result in a greater microbial inactivation (Guerrero, López-Malo, & Alzamora, 2001; López-Malo, Guerrero, & Alzamora, 1999).

2.5. Microscopic observations

Conventional microscopy techniques were used to reveal structural changes. Environmental scanning electron microscopy (ESEM), light microscopy (LM), transmission electron microscopy (TEM) and atomic force microscopy (AFM) were used to examine micro, ultra and nanostructure in ultrasound and hydrogen peroxide treated berries, while ESEM, LM and TEM were employed for micro and ultrastructure observations in UV–C irradiated berries.

For ESEM, rectangular strips (1.5 cm length, 1 cm width) of epicarp were excised, mounted on metal supports and observed using an Electroscan 2010 (Wilmington, MA, USA) Environmental Scanning Electron Microscope operating at 10.0–20.0 kV and 2.0–5.0 Torr.

For LM study, transverse ultrathin sections (1 μm thick) were stained on slide with 0.05% (w/v) toluidine blue in 2.5% (w/v) Na_2CO_3 solution (pH 11.1) for 1–6 min at 60 °C, and examined under a Zeiss Phomi III Microscope (Oberkochen, Germany). All reactive were from Merck Química Argentina S.A. (Argentina).

For TEM, the outermost region of pericarp was excised in pieces of about 1 mm^3 with a scalpel, fixed in 3% (v/v) glutaraldehyde in 0.2 M Na_2HPO_4–Na_2HPO_4 buffer solution (pH 7.4) at 4 °C for 12 h. Samples were then washed with the buffer for 24 h and postfixed in 1% (w/v) OsO_4 aqueous solution at 20 °C for 2 h. Samples were washed with the same buffer for 1 h, dehydrated in an ascending ethanol series (50% (v/v), 70% (v/v), 90% (v/v), 100% (v/v), 15 min each) and ethanol–acetone series (2:1, 2:2, 1:3; pure acetone, 15 min each) at 20 °C, and embedded in low viscosity Spurr's resin (Spurr, 1969). Ultrathin sections (1 μm thick) were cut using a glass knife with a Sorvall MT 2-B ultracut microtome, collected on copper grids and double stained with uranyl acetate and Reynolds lead-citrate (Reynolds, 1963). Sections were examined using a JEOL JEM 1200 EX II Transmission Electron Microscope (Tokyo, Japan) at an accelerating voltage of 90 kV.

For AFM, ultrathin sections were cut using a glass knife with a Sorvall MT 2-B ultracut microtome, collected unstained on cover glasses, mounted on mica disks and examined in a Multimode Atomic Force Microscope with a NanoScope III A-Quadrex controller III (Digital Instruments-Veeco, Santa Barbara, CA, USA). Topography, amplitude and phase images were acquired simultaneously by using the tapping mode under dried N_2. The AFM tips (silicon cantilevers) were 125 μm long and had a nominal spring constant of 40 N/m (TAP 300, Nano Devices, Santa Bárbara, USA). The scan area sizes varied from 15×15 μm to 1×1 μm. The scan rate applied was 1–5 Hz.

2.6. Evaluation of mechanical properties

Puncture test on whole grape was performed using an Instron Universal Testing Machine model 1011 (Canton, Massachusetts, USA) with a stainless steel plunger with a flat-end cylindrical probe (3 mm in diameter), at a deformation speed of 50 mm/min and a load range of 10 N at ambient temperature (25 ±1 °C) and 85% of relative humidity . The force was recorded every 0.33 s. Each specimen was placed on a flat steel holder (10 mm thick) with a hole (10 mm in diameter) in the center and was penetrated on the equatorial side (perpendicular to the abscission zone). This appears to be the best position for grape puncture test as supported by previous studies by Lee and Bourne (1980) and Letaief et al. (2006). From the force-displacement curve, three mechanical parameters were computed. The maximal rupture force (F_R, expressed in N) represents the force required to puncture the grape skin. The probe position at F_R (D_R, expressed in mm) indicates the deformation at the rupture point. The mechanical work (W, expressed in mJ) corresponds to the energy needed to break the skin and was estimated by the area under the curve up to the skin rupture point. Puncture measurements were performed immediately after treatments on 25 grape berries from each batch.

2.7. Color measurement

Grape berry surface color was measured with a handheld tristimulus reflectance spectrocolorimeter Model CM-508-d (Minolta Co., Japan) by using a 1.4 cm measuring aperture and a white background. Values were obtained for C illuminant and 2° observer. Before the test, the instrument was calibrated with a standard black glass and a standard white provided by the manufacturer.

The C.I.E. color coordinates (X, Y, Z) and the L*, a*, b* components of the CIELAB space were recorded, where L* indicates lightness or luminance, a* indicates chromaticity on a green (−) to red (+) axis, and b* chromaticity on a blue (−) to yellow (+) axis. These numerical values were converted into "chroma" (C) and "hue angle" (h) color functions using the following equations:

$$C = \left(a^{*2} + b^{*2}\right)^{1/2} \quad (1)$$

$$h = arctg(b*/a*) \quad (2)$$

Hue angle can be distributed in the four quadrants of the a* b* plane (red-purple: 0°, yellow: 90°, bluish-green: 180° and blue: 270°) and chroma represents the intensity or purity of the hue.

Color was evaluated in raw grape berries (control) and in treated berries immediately after processing. Ten independent samples were used for each condition with two readings taken at two different positions in the equatorial zone of each fruit. The reported results were based on the average value.

2.8. Statistical analysis

Statistical analyses were carried out using InfoStat Versión 2009 (InfoStat Group, FCA, UNC, Córdoba, Argentina). Mechanical and color data were analyzed by multivariate analysis of variance (MANOVA) (Quinn & Keough, 2002). Three and five response variables were taken from mechanical and color analysis, respectively. Post-hoc multiple comparisons among multivariate means of treatments were performed by Hotelling tests based on Bonferroni correction. Discriminant function analysis (DFA) was applied as an extension of multivariate analysis of variance (McGarigal, Cushman, & Stafford, 2000). Previously to conduct the analyses, the assumptions of homogeneity of variance–covariance matrices and multivariate normal distribution were tested. Multivariate outliers were detected by Mahalanobis distance and removed from data set. Multicolinearity among response variables was assessed by the Pearson correlation matrix, and only uncorrelated variables were entered into the MANOVA and DFA analyses. Values of $P<0.05$ were considered to be significant in all analyses.

3. Results and discussion

3.1. Microscopic features

3.1.1. Raw grape berries

Raw grape berries, between 15 and 20 mm in diameter, were grayish blue, turgent and rounded in shape. Epicarp exhibited intact and uniform general aspect, with epicuticular waxes that determined their dull surface.

With ESEM and in superficial view, the epicarp of raw fruits appeared as a striated to irregularly reticulated layer. Waxes (like platelets) were arranged in emergent and oblique plates distributed all over the surface (Fig. 1: A).

LM analysis showed the epicarp composed by one stratum of epidermis and three or four subepidermic collenchymatous layers. In general, epidermal cells exhibited rectangular shape, parietal cytoplasm, turgent central vacuole with tannin and anthocyanin contents, thick outer tangential walls, and thinner radial and inner walls. Mesocarp (edible pulp) presented evident intercellular spaces, and rounded to irregular turgent cells with parietal cytoplasm (Fig. 2: A–B).

TEM study of the outer tangential epidermal cell walls showed the epicuticular waxes as a translucent stratum with a sinuous superficial contour. Cuticle, about 0.7–1 μm thick, appeared well defined, amorphous, and with irregular contour. In addition, a gradual delimitation between cuticle and cutinized layer was observed (Fig. 3: A). Cutinized layer, about 2.2–2.6 μm thick, was electron dense, exhibited reticulated pattern and an abrupt transition with non cutinized cellulose layer (Fig. 3: A). Non cutinized cellulose layer, electron-dense, about 1.5 μm thick, showed the cellulose microfibrils with a longitudinal pattern, distributed parallel to the surface (Fig. 3: B). Epidermal cells presented parietal cytoplasm, and vacuole with tannin and anthocyanins (Fig. 3: B).

AFM observations (topography and amplitude image types) taken at 5×5 μm area revealed the slightly undulated contour of epicuticular waxes and the loose cuticular membrane (Fig. 4: A–B). Topography image type of the cuticular membrane (2×2 μm area) showed the outermost region with nanopores, radially extended, and intermixed between zones of cutin and polysaccharides (Fig. 4: C).

Topography and amplitude image types of non cutinized cellulose layer showed microfibrils distributed in an evident layered pattern. Three-dimensional image (1×1 μm area) corroborated the following features: visible and parallel thick layers, evident spacing between layers, high spatial frequency of cellulose aggregates, cellulose aggregate irregular in shape, and variable in size, nanopores, conspicuous, irregular, and narrow to slender (Fig. 5: A–C, Fig. 6: A–B).

3.1.2. Hydrogen peroxide treated grape berries

In superficial view, treated grapes presented a general aspect similar to the control one: dark blue color, round shape, uniform intact epicarp, and firm consistence.

With ESEM, the surface of both epicuticular wax and cuticle layers showed a conspicuous striated pattern intermixed with small, irregular, and occasional smooth areas (Fig. 1: B).

LM observations of transverse sections revealed the epicarp composed by one stratum of epidermis, and four subepidermic collenchymatous layers. In general, the structure of grapes undergone hydrogen peroxide treatment was similar to the control one, corroborating that the effect of the sanitizer was mainly at surface level (Fig. 2: C–D).

TEM study showed a slight thickness increase in both epicuticular wax, and cuticle proper layers (Fig. 3: C). In addition, epicuticular wax layer (Fig. 3: C) appeared with undulated contour and a slight delimitation between cuticle and cutinized layer was observed. After treatment, electron dense polysaccharides of the cutinized layer

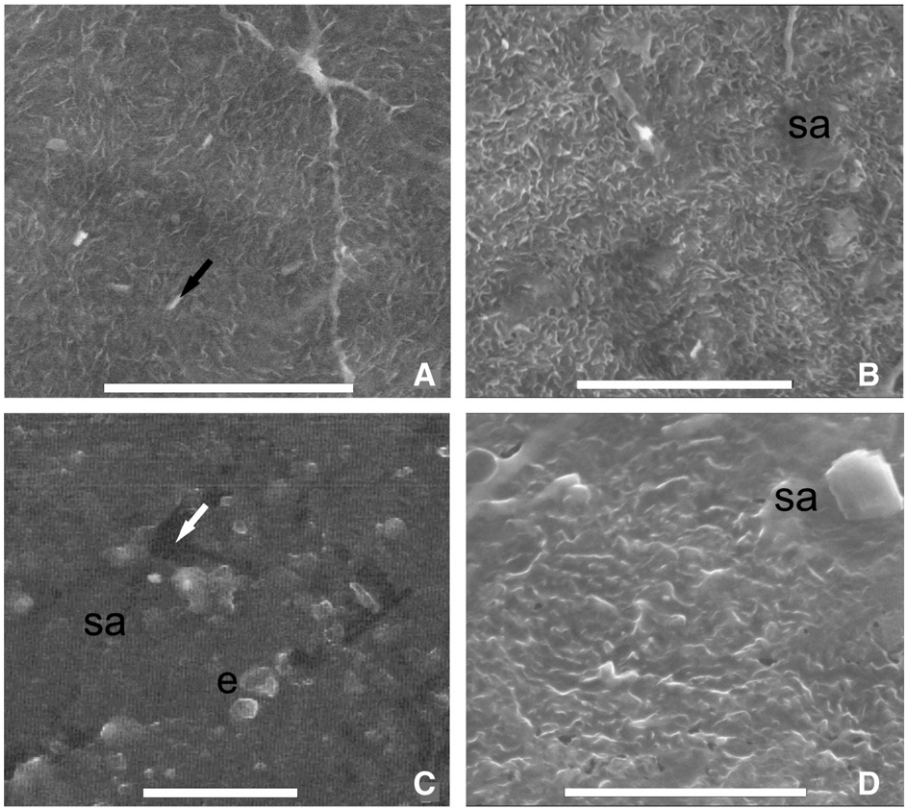

Fig. 1. *V. labrusca* L., ESEM micrographs, epicarp (superficial views). A, Raw grape; B, hydrogen peroxide treated grape; C, UV-C treated grape; D, ultrasound treated grape. Black arrow = oblique plates; e = excrescences; sa = smooth areas; white arrow = disruption. Scales: A, C and D = 25 μm; B = 30 μm.

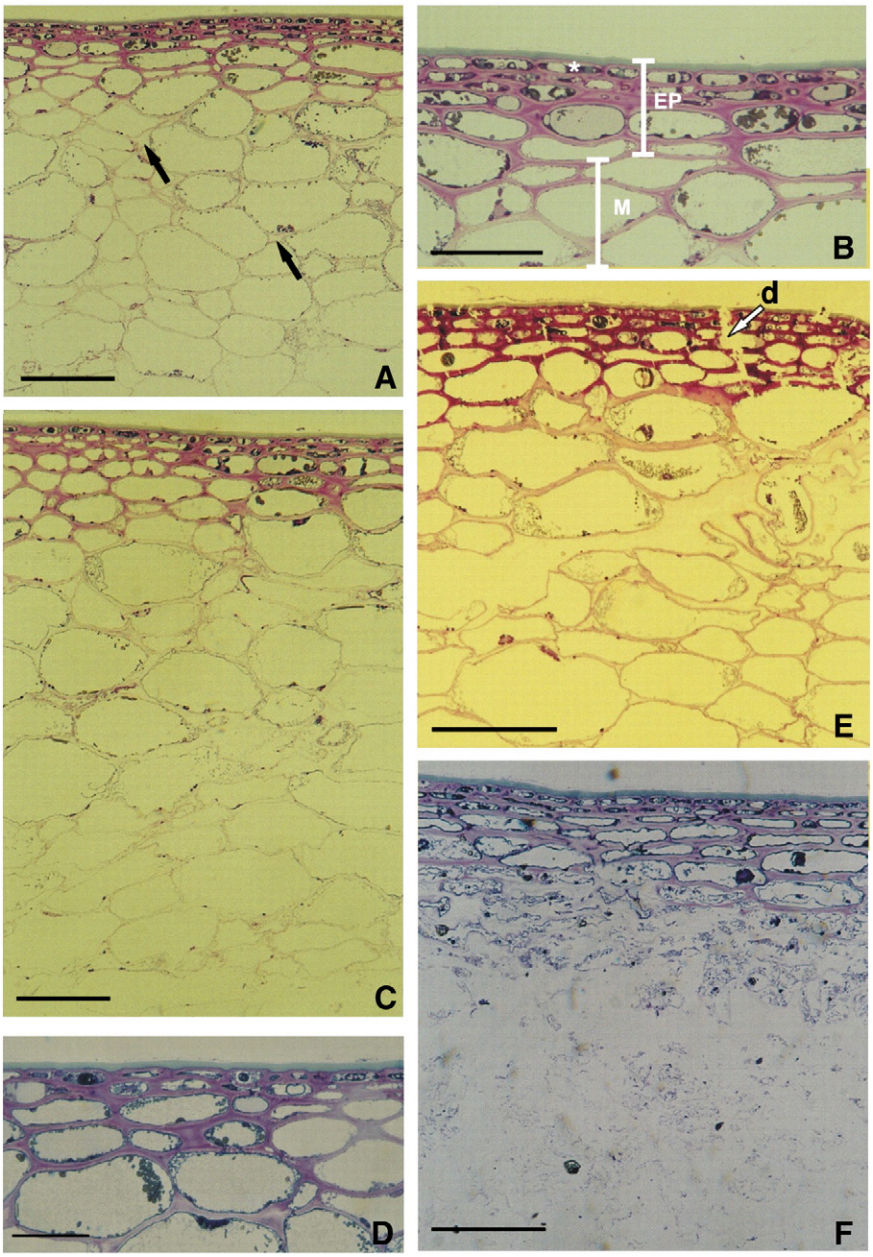

Fig. 2. *V. labrusca* L., LM micrographs, epicarp and mesocarp (transverse sections). A and B, Raw grapes: A, epicarp and mesocarp, general aspect; B, epicarp, detail; C and D, hydrogen peroxide treated grapes; E, UV-C irradiated grape; F, ultrasound treated grape. Black arrow = intercellular space; d = disruptions; EP = epicarp; M = mesocarp; white asterisk = tannin and anthocyanin contents. Scales: A, C, E and F = 100 μm; B and D = 50 μm.

acquired a more packed reticulated pattern (Fig. 3: C). Besides, an abrupt transition between cutinized layer, and non cutinized cellulose layer was exhibited (Fig. 3: C–D). Electron dense non cutinized cellulose layer showed a slight altered pattern distribution of crowded or packed cellulose microfibrils (Fig. 3: D).

AFM observations (topography and amplitude image types) taken at 8 × 8 μm area revealed the epicuticular wax layer with a conspicuously undulated contour characterized by a high frequency of folding (Fig. 4: D–E). The outermost region of the cuticular membrane (CM) appeared more compacted respect to the control one (Fig. 4: D–E). Topography image type of the cuticular membrane (4 × 4 μm area) exhibited the loose middle and innermost region with numerous and irregular nanopores (Fig. 4: F).

Topography and amplitude images of non cutinized cellulose layer showed a layered distribution pattern of cellulose microfibrils. Three-dimensional image (1 × 1 μm area) documented the more compacted cellulose layers with narrow spacing between layers (Fig. 5: D–F). Furthermore, phase image exhibited cellulose aggregates with increased spatial frequency and regular pattern. Nanopores appeared narrow to elongate (Fig. 6: C).

3.1.3. Ultrasound treated grape berries

In superficial view treated grapes were rounded in shape and intense blue colored. All fruits exhibited intact epicarp and firm consistence. Detected alterations were related to the presence of areas without a dull surface.

With ESEM, the epicarp surface exhibited a conspicuous striated pattern, intermixed with irregularly extended smooth areas (Fig. 1: D).

LM observations revealed slight epicarp compression, plasmolysis of subepidermal cells, and mesocarp collapse (Fig. 2: F).

TEM study of treated grapes confirmed alteration of epicuticular wax and non cutinized cellulose layers. In transverse section epicuticular wax layer showed accentuated and irregular serrated contour (Fig. 3: G). Transitions between layers (epicuticular wax,

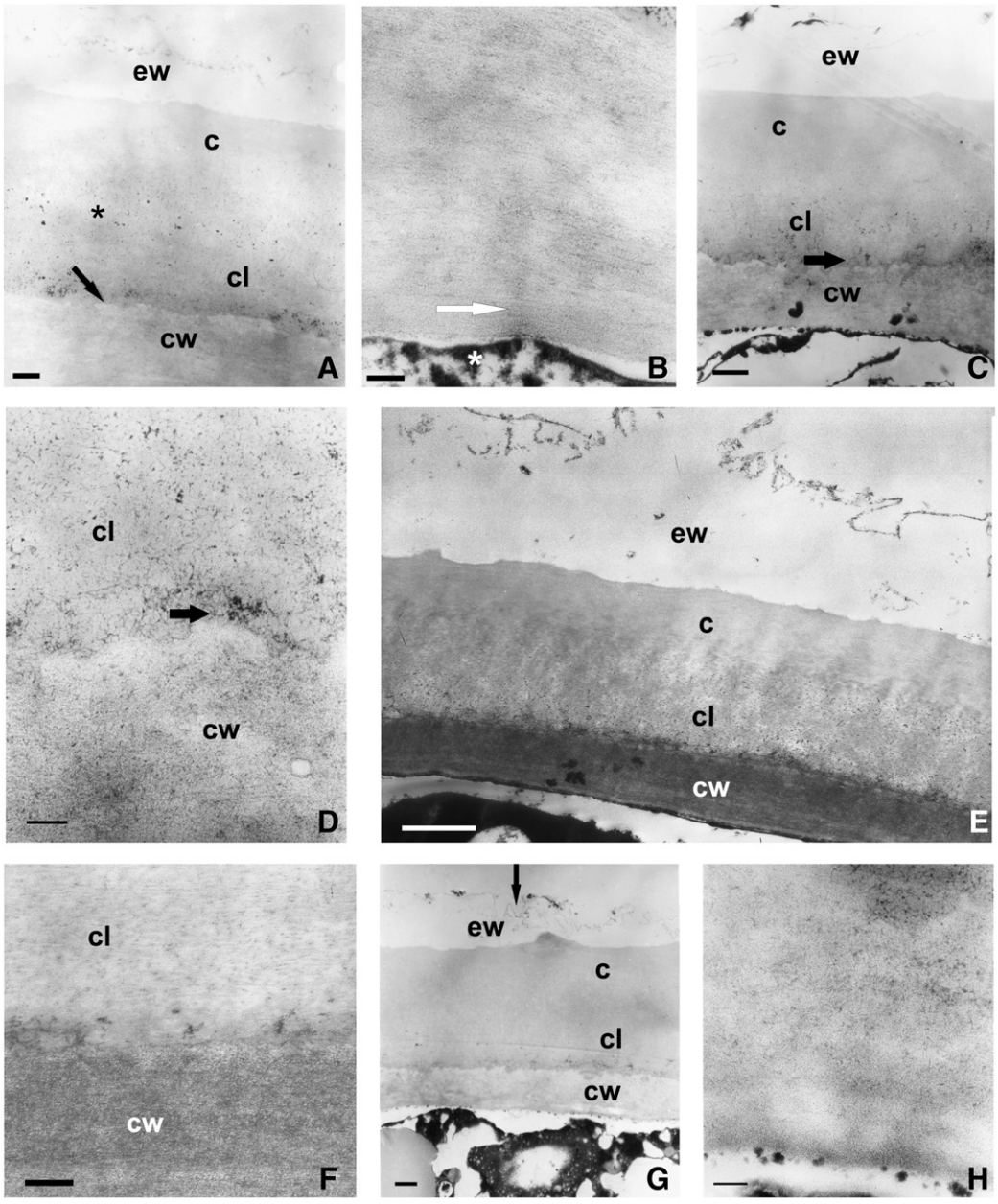

Fig. 3. *V. labrusca* L., TEM micrographs (transverse sections). A and B, Raw grapes: A, outer tangential epidermal cell wall, general aspect; B, non cutinized cellulose layer; C and D, hydrogen peroxide treated grapes; E and F, UV-C treated grapes; G and H, ultrasound treated grapes. Black arrow = delimited transition between cl and cw; black asterisk = slight transition between c and cl; c = cuticle; cl = cutinized layer; cw = non cutinized cellulose layer; ew = epicuticular wax layer; white arrow = cellulose microfibrils parallel pattern; white asterisk = vacuole with tannin and anthocyanin contents. Scales: C, E and G = 1 μm; A = 500 nm; B, D, F and H = 200 nm.

cuticle proper, cutinized layer, and non cutinized cellulose layer) appeared similar to the control one. Non cutinized cellulose layer had an altered pattern distribution. Some packed cellulose microfibrils (electronically dense areas) appeared intermixed between translucent zones (Fig. 3: G–H).

AFM observations (topography, and amplitude image types) taken at 15 × 15 μm area exhibited the altered epicuticular wax layer with serrated contour (Fig. 4: G–H). Likewise, topography image (5 × 5 μm area) showed the more compacted cutinized layer (Fig. 4: I).

Topography and amplitude image types of non cutinized cellulose layer revealed an evident layered pattern alteration (Fig. 5: G–H) Topography, amplitude, and three-dimensional image (1 × 1 μm areas) corroborated the presence of visible, parallel, thick and wrinkled non cutinized cellulose layers. The spacing between layers was apparently similar to the control one (Fig. 5: G-I). Phase image types exhibited cellulose aggregates with high frequency, irregular in shape, variables in size, and intermixed between twisted nanopores (Fig. 6: D).

3.1.4. UV–C light treated grape berries

Treated grapes presented a general aspect similar to the control one. They appeared rounded in shape, intense blue colored, with intact epicarp and firm consistence.

With ESEM the surface was observed markedly altered respect to the control one. In general, it showed more smooth areas intermixed with irregular disruptions and excrescences. Excrescences appeared variables in shape, and randomly distributed (Fig. 1: C).

LM observations of UV–C irradiated fruits reported signs of epicarp alterations. In transverse section, outer and inner tangential epidermal cell walls and cell walls of the three–four collenquimatous subepidermal layers appeared disrupted. Mesocarp exhibited a general aspect similar to the control ones (Fig. 2: E).

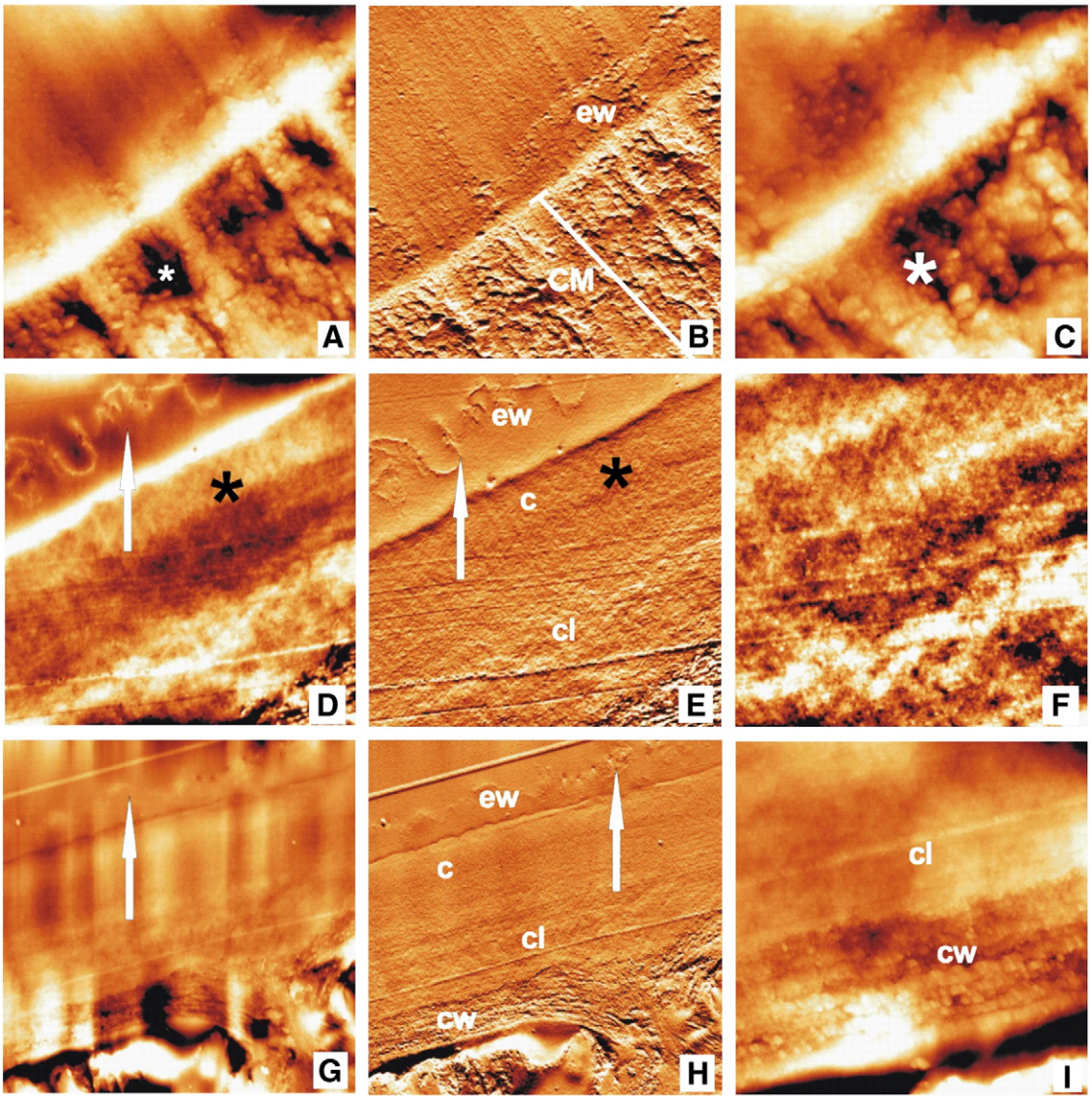

Fig. 4. *V. labrusca* L., AFM micrographs. A—C, Raw grapes, epicuticular wax layer, and cuticular membrane; A and B topography and amplitude image types, respectively; C, topography image type; D—F, hydrogen peroxide treated grapes; s: DE, epicuticular wax layer, and cuticular membrane; topography and amplitude image types, respectively; F, cutinized layer, topography image type; G—I, ultrasound treated grapes: G and H, outer tangential epidermal cell wall: topography and amplitude image types, respectively; I, cutinized and non cutinized cellulose layers, topography image type. Black asterisk = compact cuticle; c = cuticle; cl = cutinized layer; CM = cuticular membrane; cw = non cutinized cellulose layer; ew = epicuticular wax layer; white arrow = ew contour; white asterisk = nanopore. Scan sizes: A and B, I = 5 × 5 μm; C = 2 × 2 μm; D and E = 8 × 8 μm; F = 4 × 4 μm; G–H = 15 × 15 μm.

TEM study showed abrupt transition between all layers (epicuticular wax, cuticle proper, cutinized layer, and non cutinized cellulose layer) of the outer tangential epidermal cell wall (Fig. 3: E). Electron less dense polysaccharides of the cutinized layer appeared with a reticulated pattern. Non cutinized cellulose layer, markedly electron dense, exhibited conspicuously packed cellulose microfibrils with an altered pattern distribution. Cellulose microfibrils appeared parallel to the surface, and occasionally intermixed between others with different orientation (Figs. 3: E–F).

3.2. Mechanical properties

Typical force-deformation curves after puncturing of grape berries are shown in Fig. 7. Samples exhibited very similar mechanical behavior regardless of the treatment. The curves presented one fracture peak followed by an abrupt fall in force. Mean values of mechanical parameters (rupture force, F_R; deformation at the rupture point, D_R, and mechanical work, W) are exhibited in Table 1.

The force-deformation curves resulted similar to V. *lambruscana* Bailey cultivar profiles published by Sato, Yamanez, Hirakawa, Otobe, and Yamada (1997). Although puncture test takes into account the behavior of the whole fruit (Maury et al., 2009), it can be observed in Fig. 7 that the skin of grape berries (treated or untreated) had the major effect on the mechanical properties, contributing more than 80% of the firmness of the fruit before the rupture point. The minor role of the penetrating force in the flesh (lower than 20% of the rupture force) had also been reported in unpeeled tomato, cucumber, Japanese pear and apple (Jackman & Stanley, 1994; Sirisomboon, Tanaka, Akinaga, & Kojima, 2000; Thompson, Fleming, & Hamann, 1992).

MANOVA results indicated that treatment effects did not vary significantly (MANOVA; treatment $F_{6,\ 192} = 1.79$; $P = 0.1037$). The first discriminant function derived from DFA accounted for most of the variation (77.98%), whereas the second discriminant function accounted for little variation (22.02%). Coincidently with MANOVA results, not any response variable was significant to discriminate and consequently to generate clusters of treatments (Fig. 8). DFA only correctly classified the treatments of 34% (n = 100) of the random grape berries test data. Raw grapes and UV–C treatment (40% and 56%, respectively) were better classified than ultrasound (36% correctly

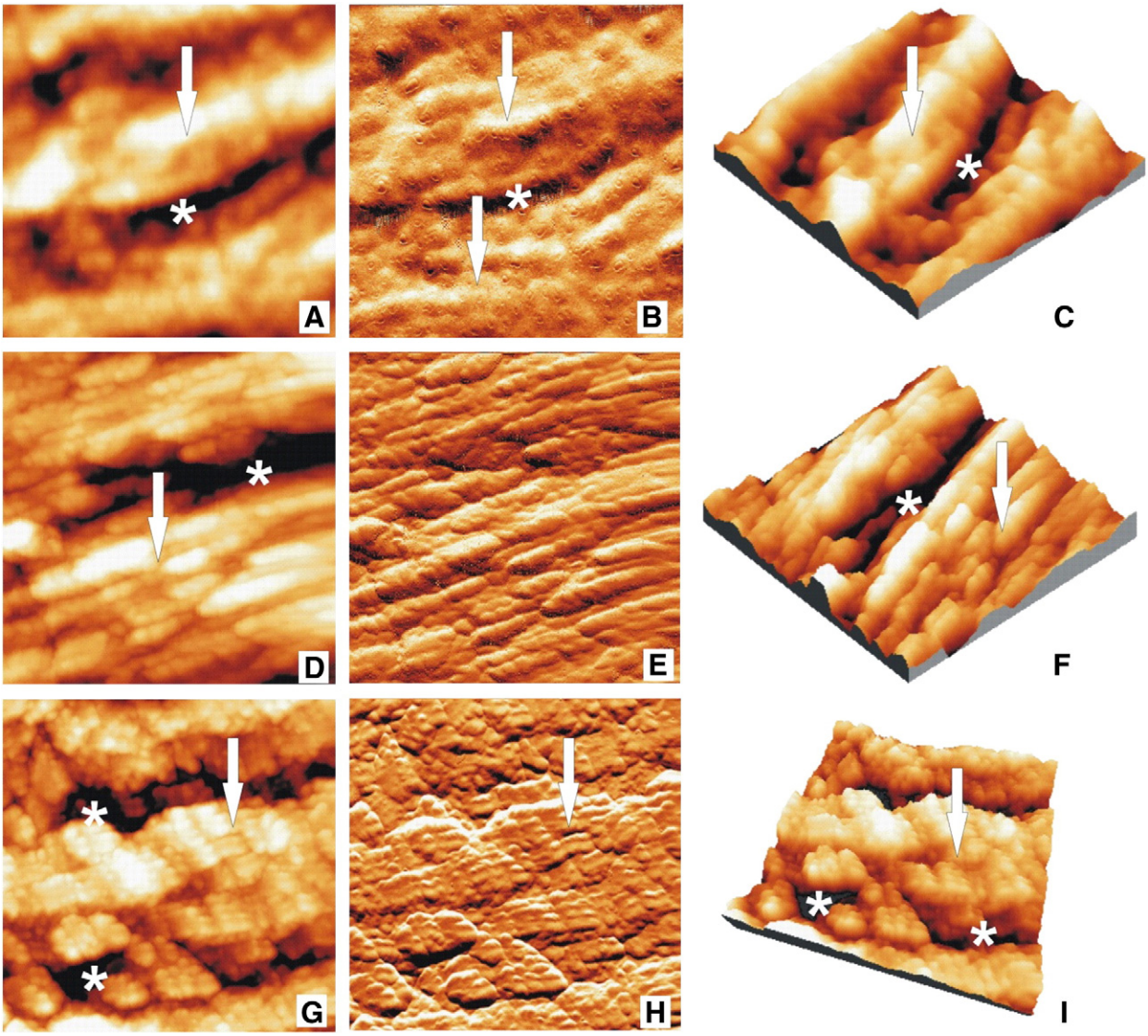

Fig. 5. *V. labrusca* L., AFM micrographs of non cutinized cellulose layer: topography, amplitude, and 3-D image types. A–C, Raw grapes; D–F, hydrogen peroxide treated grapes; G–I, ultrasound treated grapes. White arrow = cellulose layer; white asterisk = nanopore. Scan sizes: A—I = 1 × 1 μm.

classified) and hydrogen peroxide (4% correctly classified) treatments. The DFA was unsuccessful because it was impossible to discriminate treatments.

3.3. Color

The values of colorimetric average L*, a* and b* parameters and of C and h functions of grape berries subjected to the different treatments are presented in Table 2. The one-way MANOVA of treatments was highly significant for color measurements ($F_{15, 102} = 4.42$; $P < 0.0001$). Treatment group centroids were statistically different as the result of post-hoc multiple comparisons (Hotelling tests $P < 0.05$), although multivariate means of both UV–C and hydrogen peroxide treatments did not differ statistically (Table 2).

Ultrasound treatment resulted in a decrease in L* and C and in an increase in a*, b* and h mean values. The decrease in L* and C and the increase in h mean values indicated that treated grape surface became darker and take a more purple and dull color. Hydrogen peroxide and UV–C treatments also decreased lightness.

The first discriminant function resulted from DFA explained most of the between-groups (raw and treatments) variance (87.12%), whereas the second discriminant function explained the little variation remaining (10.97%). In grapes, the most important discriminating selective variables among treatments were lightness (L*), chromaticity on a blue to yellow axis (b*) and chroma (C*), which contributed most to the first and the second discriminant functions (Fig. 9). The 85% (n = 40) of random grape berries were successfully classified by treatments from DFA. The percentage of successful prediction was perfect for ultrasonic treatment and raw berries (100% each one), followed by hydrogen peroxide treatment (80% correctly classified) and UV–C treatment (60% correctly classified).

3.4. Relationship between structure and mechanical and color parameters

In relation to LM structural alterations, after hydrogen peroxide treatment, grape berries appeared similar to the raw fruit. Ultrasound generated a slight epicarp compression, subepidermal cells plasmolysis, and mesocarp collapse. UV–C radiation impacted over the epicarp, causing the disruption of some outer and inner tangential epidermal and subepidermal cell walls. ESEM observations confirmed that all treatments applied (ultrasound, hydrogen peroxide and UV–C) caused ultrastructural changes in epicuticular waxes and only UV–C radiation caused epicarp cell wall disruption. Changes analyzed with TEM confirmed that all treatments altered the epicuticular waxes

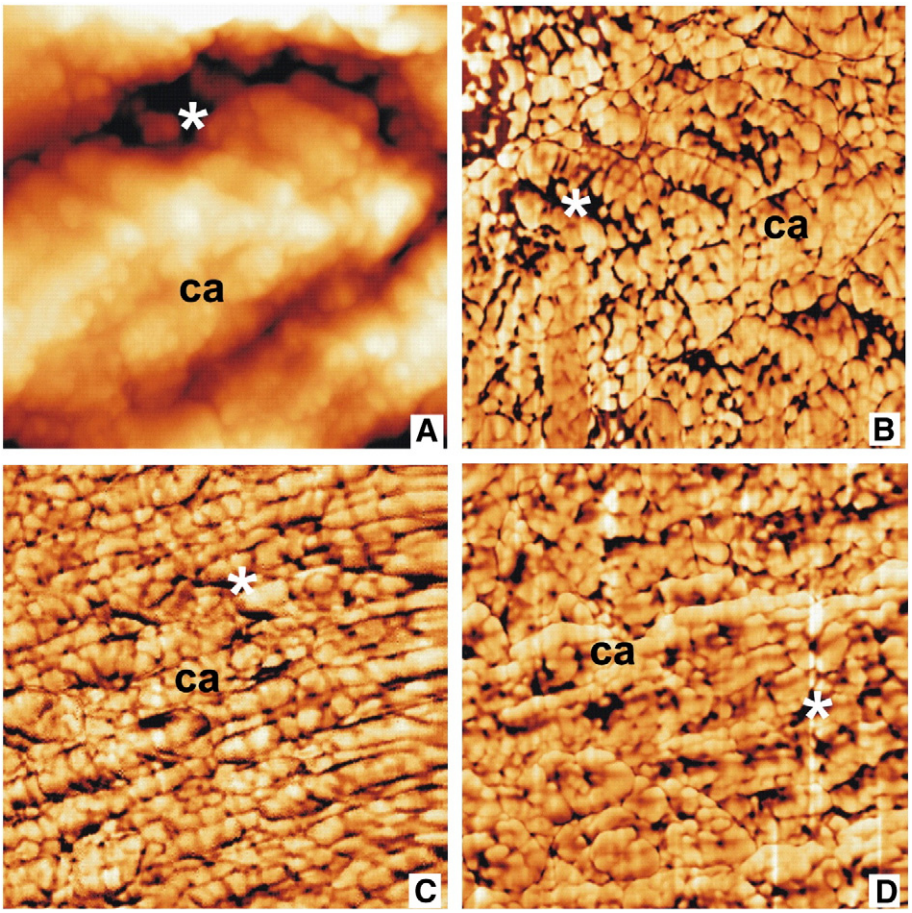

Fig. 6. *V. labrusca* L., AFM micrographs of non cutinized cellulose layer (cellulose aggregates): A and B, Raw grapes: topography and phase image types, respectively; C and D, phase image types: C, hydrogen peroxide treated grape; D, ultrasound treated grape. ca = cellulose aggregate; white asterisk = nanopore. Scan sizes: A–D = 1 × 1 μm.

ultrastructure, accentuated the non cutinized cellulose layer and the cuticular membrane transition, and maintained the gradual transition between the cutinized layer and the cuticle proper. AFM structure study showed that ultrasound and hydrogen peroxide treatments affected the nanostructure of outer tangential epidermal cell wall, generating changes in the layered cellulose domain, compressing the cellulose layer and altering the cellulose aggregate and nanofracture morphology. While ultrasound compressed the cuticular membrane, hydrogen peroxide treatment maintained the cutinized layer porosity and only compressed the cuticle. The nanoporosity caused by hydrogen peroxide treatment in the non cutinized cellulose layer would confirm the finding reported by Miller (1986). This author mentioned the oxidation of cell wall polysaccharides by hydrogen peroxide treatment as a potential mechanism for cell wall breakdown in plants.

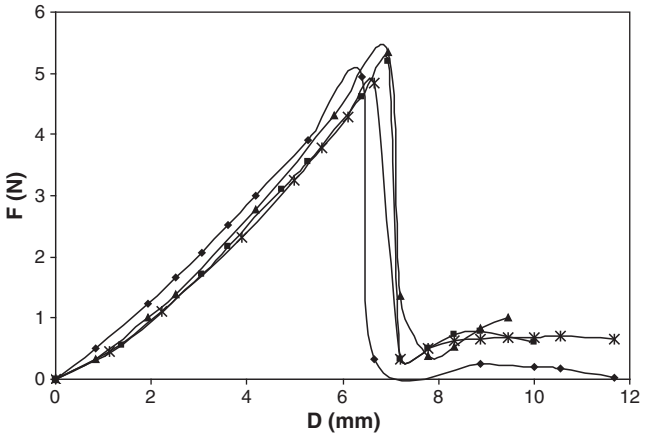

Fig. 7. Typical penetrometric force—displacement curves for raw and treated grape berries. ♦ Raw grape; ■ hydrogen peroxide treated grape; ▲ UV–C treated grape; x ultrasound treated grape.

Cellular structure is a predominant factor in determining the mechanical behavior of plant tissues. Molecular, microscopic (nano, ultra and microstructure) and macroscopic features of the tissues are usually paralleled with functional properties (Sila et al., 2008). As it is observed in Fig. 7, fruit skin played a great role in the overall firmness and puncture test was more linked to the skin rheological characteristics. Accordingly, alterations in skin architecture would be undoubtedly important on puncture response of treated grape berries. However, statistical analysis did not reveal significant differences in the mechanical behavior between treated and raw fruits. Apparently structural and nanostructural alterations observed after treatments would not be enough to be detected in grape berry puncture tests.

It is interesting to mention that the similarity of raw and treated grapes force-deformation profiles was concordant with DFA impossibility to discriminate treatments. The low impact on mechanical

Table 1
Mean value ± SD (standard deviation) of F_R, D_R and W parameters for raw and treated grape berries.

Treatment	F_R (N) ± SD	D_R (mm) ± SD	W (mJ) ± SD
Raw grapes	4.9 ± 0.2	6.0 ± 0.2	13.4 ± 0.8
Hydrogen peroxide	5.2 ± 0.1	6.4 ± 0.1	14.5 ± 0.5
UV–C	5.4 ± 0.2	6.5 ± 0.1	15.2 ± 0.7
Ultrasound	4.9 ± 0.1	6.2 ± 0.1	13.1 ± 0.6

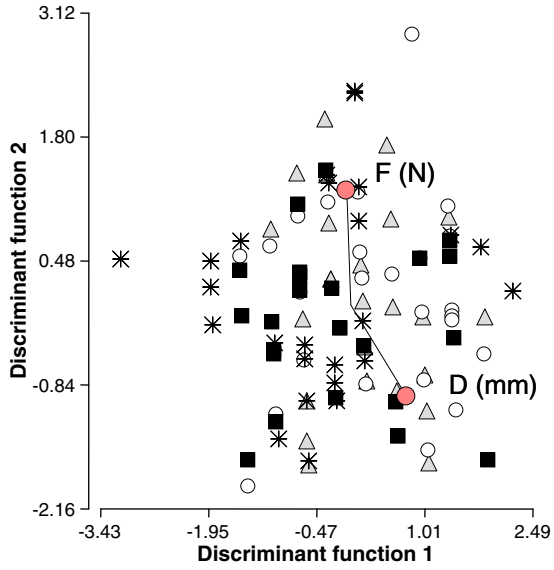

Fig. 8. Puncture test data statistical analysis. Canonical scores for the first two discriminant functions derived from measurements and two variables. Raw (✳) and UV–C (○), ultrasound (■) and hydrogen peroxide (▲) treated grapes.

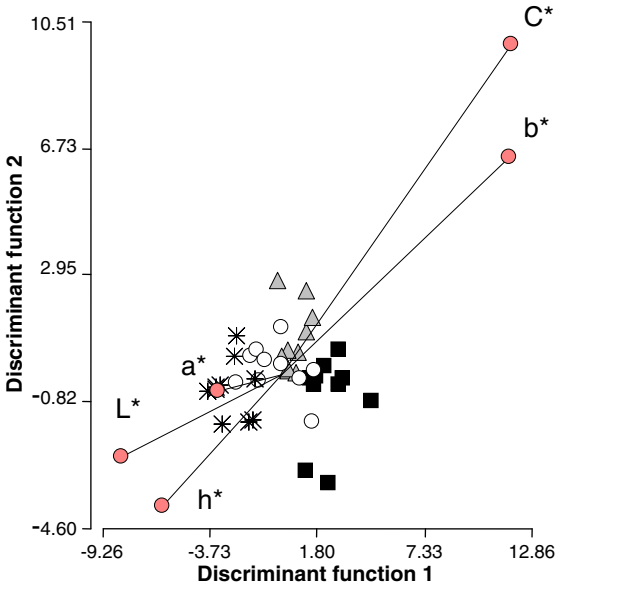

Fig. 9. Colour data statistical analysis. Canonical scores for the first two discriminant functions derived from measurements and five variables. Raw (✳) and UV–C (○), ultrasound (■) and hydrogen peroxide (▲) treated grapes.

properties would support the application of these emerging techniques for grape berry decontamination in terms of texture quality, at least in the assayed doses.

Color statistical analyses revealed significant differences among treated and raw grapes. All chemical and physical treatments assayed altered the epicuticular wax layer of grapes. These changes would be directly related to L* color parameter. Microscopic information revealed that the epicuticular wax structural modification was very severe in ultrasound treated grapes, which exhibited the major differences in lightness as compared to raw fruit. Changes in epicuticular waxes of fruits undergone hydrogen peroxide and UV–C radiation would be not so different to support significant differences between both treatments. On the other side, the more purple color of ultrasound treated grapes could be ascribed to the extraction of anthocyanins by alteration of membranes (tonoplast and plasmalemma) and cell walls (Fig. 2F).

4. Conclusions

Epicarp disruption, cell plasmolysis, mesocarp collapse, epicuticular wax layer pattern alteration, accentuated transition between cellulose layer and cuticular membrane of the outer tangential epidermal cell wall, cellulose aggregates with peculiar pattern organization and nanofractures, variables in shape and size, were some of the structure features corroborated after ultrasound, hydrogen peroxide and UV–C light treatments. The color of grape berries was slightly but significantly affected by the decontamination procedures while mechanical properties determined by puncture test did not vary.

Table 2
Mean value ± SD (standard deviation) of L*, a* and b* parameters, and C, and h functions for raw and treated grape berries.

Treatment	L* ± SD	a* ± SD	b* ± SD	C ± SD	h ± SD	
Raw grapes	34.5 ± 2.7	0.7 ± 0.5	−3.9 ± 0.6	4.0 ± 0.5	281.1 ± 4.3	A
UV–C	32.2 ± 2.2	0.5 ± 0.2	−3.8 ± 0.6	3.9 ± 0.6	277.2 ± 3.4	C
Hydrogen peroxide	30.9 ± 1.1	0.8 ± 0.8	−4.0 ± 0.5	4.2 ± 0.5	280.8 ± 9.0	C
Ultrasound	26.1 ± 2.8	0.9 ± 0.5	−2.7 ± 0.9	3.0 ± 0.6	292.6 ± 18.0	B

Post-hoc multiple comparisons using Hotelling tests based on Bonferroni correction $\alpha = 0.05$.
Different letters indicate significant differences at $P \leq 0.05$.

The low impact of structural changes on mechanical and color characteristics would indicate the potential of the assayed treatments as innovative decontamination techniques for grape berry preservation, at least at the assayed doses. The different UV–C and hydrogen peroxide applied doses were selected based on previous literature reports and on our preliminary assays in order to reduce microbial load on different fruits. Ultrasound conditions were chosen taken into account the maximum dose that did not provoked adverse visual effects. Present results contribute to understand the structural changes caused by the treatments *per se*. Finding the best conditions, doses and combination treatments for different hurdle decontamination technologies is a further challenge for the commercial adoption of these technologies.

Future research is encouraged to investigate not only the effect of the treatments after processing but also the influence along storage to get a better evaluation of the shelf-life of grapes decontaminated by the assayed techniques.

Acknowledgements

The authors acknowledge the valuable AFM technical assistance of Silvio Ludueña from CMA-FCEyN-UBA, and the financial support from the University of Buenos Aires, CONICET, and ANPCyT of Argentina and from BID.

References

Allende, A., Tomás-Barberán, F. A., & Gil, M. I. (2006). Minimal processing for healthy traditional foods. *Trends in Food Science and Technology*, *17*, 513–519.
Baker, E. A. (1982). Chemistry and morphology of plant epicuticular waxes. In D. F. Cutler, K. L. Alvin, & C. E. Price (Eds.), *The plant cuticle. Linnean Society Symposium Series*, *Vol. 10*. (pp. 139–165) London: Academic Press.
Beuchat, L. R. (2000). Use of sanitizers in raw fruit and vegetable processing. In S. M. Alzamora, M. S. Tapia, & A. López Malo (Eds.), *Minimally processed fruits and vegetables. fundamental aspects and applications* (pp. 63–78). Gaithersburg, Maryland: Aspen Publishers, Inc.
Carpita, N. C., & Gibeaut, D. M. (1993). Structural models of primary cell walls in flowering plants: Consistency of molecular structure with the physical properties of the walls during growth. *The Plant Journal*, *3*, 1–30.
Carreño, J., Martínez, A., Almela, L., & Fernández-López, J. A. (1995). Proposal of and index for the objective evaluation of the colour of red table grapes. *Food Research International*, *28*, 373–377.
Casado, C. G., & Heredia, A. (2001). Ultrastructure of the cuticle during growth of the grape berry (*Vitis vinifera* L.). *Physiologia Plantarum*, *111*, 220–224.

Cosgrove, D. J. (2001). Wall structure and wall loosening. A look backwards and forwards. *Plant Physiology*, *125*, 131–134.
Esau, K. (1977). *Anatomy of seed plants* (2nd ed.). New York: J. Wiley and Sons.
Fernández-López, J. A., Almela, L., Muñoz, J. A., Hidalgo, V., & Carreño, J. (1999). Dependence between colour and individual anthocyanin content in ripening grapes. *Food Research International*, *31*, 667–672.
Gardner, D. W., & Shama, G. (2000). Modeling UV-induced inactivation of microorganisms on surfaces. *Journal of Food Protection*, *63*, 63–70.
González-Paramás, A. M., Esteban-Ruano, S., Santos-Buelga, C., de Pascual-Teresa, S., & Rivas-Gonzalo, J. C. (2004). Flavonol content and antioxidant activity in winery byproducts. *Journal of Agricultural and Food Chemistry*, *52*, 234–238.
Guerrero, S. N., López-Malo, A., & Alzamora, S. M. (2001). Effect of ultrasound on the survival of *Saccharomyces cerevisiae*. Influence of temperature, pH and amplitude. *Innovative Food Science and Emerging Technologies*, *2*, 31–39.
Holloway, P. J. (1982). The chemical constitution of plant cutins. In D. F. Cutler, K. L. Alvin, & C. E. Price (Eds.), *The plant cuticle. Linnean Society Symposium Series*, *Vol. 10*. (pp. 45–85) London: Academic Press.
Huang, X. M., Huang, H. B., & Wang, H. C. (2005). Cell walls of loosening skin in post-veraison grape berries loose structural polysaccharides and calcium while accumulate structural proteins. *Scientia Horticulturae*, *104*, 249–263.
Jackman, R. L., & Stanley, D. W. (1994). Influence of the skin on puncture properties of chilled and nonchilled tomato fruit. *Journal of Texture Studies*, *25*, 221–230.
Jeffree, C. E., Baker, E. A., & Holloway, P. J. (1976). Origins of the fine structure of plant epicuticular waxes. In C. H. Dickinson, & T. F. Preece (Eds.), *Microbiology of aerial plant surface* (pp. 119–158). London: Academic Press.
Lee, C. Y., & Bourne, M. C. (1980). Changes in grape firmness during maturation. *Journal of Texture Studies*, *11*, 163–171.
Letaief, H., Rolle, L., Zeppa, G., & Gerbi, V. (2006). Grape skin and seeds hardness assessment by texture analysis. IUFoST. http://iufost.edpsciences.org 1847–1856.
López-Malo, A., Guerrero, S., & Alzamora, S. M. (1999). *Saccharomyces cerevisiae* thermal inactivation kinetics combined with ultrasound. *Journal of Food Protection*, *62*, 1215–1217.
Marquenie, D., Michiels, C. W., Geeraerd, A. H., Schenk, A., Soontjens, C., Van Impe, J. F., et al. (2002). Using survival analysis to investigate the effect of UV–C and heat treatment on storage of strawberry and sweet cherry. *International Journal of Food Microbiology*, *73*, 187–196.
Maury, C., Madieta, E., Le Moigne, M., Mehinagic, E., Siret, R., & Jourjon, F. (2009). Development of a mechanical texture test to evaluate the ripening process of Cabernet Franc grapes. *Journal of Texture Studies*, *40*, 511–535.
McGarigal, K., Cushman, S., & Stafford, S. (2000). *Multivariate statistics for wildlife and ecology research*. New York: Springer-Verlag.
Miller, A. R. (1986). Oxidation of cell wall polysaccharides by hydrogen peroxide: A potential mechanism for cell wall breakdown in plants. *Biochemical and Biophysical Research Communications*, *141*(1), 238–244.
Nigro, F., Hipólito, A., & Lima, G. (1998). Use of UV–C light to reduce *Botrytis* storage rot of table grapes. *Postharvest Biology and Technology*, *13*, 171–181.
Pinelo, M., Arnous, A., & Meyer, A. S. (2006). Upgrading of grape skins: Significance of plant cell-wall structural components and extraction techniques for phenol release. *Trends in Food Science and Technology*, *17*, 579–590.
Quinn, G. P., & Keough, M. J. (2002). *Experimental design and data analysis for biologists*. New York: Cambridge University Press.
Radler, F., & Horn, D. H. S. (1965). The composition of grape cuticle wax. *Australian Journal of Chemistry*, *18*, 1059–1069.
Raffellini, S., Guerrero, S., & Alzamora, S. M. (2008). Effect of hydrogen peroxide concentration and pH on inactivation kinectics of *Escherichia coli*. *Journal of Food Safety*, *28*, 514–533.
Rahn, R. O. (1997). Potassium iodide as a chemical actinometer for 254 nm radiation: Use of iodate as an electron scavenger. *Photochemistry and Photobiology*, *66*(4), 450–455.
Reynolds, E. S. (1963). The use of lead citrate at high pH as an electron opaque stain in electron microscopy. *The Journal of Cell Biology*, *17*, 208.
Rosenquist, J. K., & Morrison, J. C. (1988). The development of the cuticle and epicuticular wax of the grape berry. *Vitis*, *27*, 63–70.
Sato, A., Yamanez, H., Hirakawa, N., Otobe, K., & Yamada, M. (1997). Varietal differences in the texture of grape berries measured by penetration tests. *Vitis*, *36*(1), 7–10.
Sila, D. N., Duvetter, T., De Roeck, A., Verlent, I., Smout, C., Moates, G. K., et al. (2008). Texture changes of processed fruits and vegetables: Potential use of high-pressure processing. *Trends in Food Science and Technology*, *19*(6), 309–319.
Sirisomboon, P., Tanaka, M., Akinaga, T., & Kojima, T. (2000). Evaluation of the textural properties of Japanese pear. *Journal Texture Studies*, *31*, 665–677.
Spurr, A. R. (1969). Low-viscosity epoxy resin embedding medium for electron microscopy. *Journal of Ultrastructure Research*, *26*, 31–43.
Thompson, R. L., Fleming, H. P., & Hamann, D. D. (1992). Delineation of puncture forces for exocarp and mesocarp tissues in cucumber fruit. *Journal of Texture Studies*, *23*, 169–184.
Wattendorff, J., & Holloway, P. J. (1980). Studies on the ultrastructure and histochemistry of plant cuticles: the cuticular membrane of *Agave americana* L. *in situ*. *Annals of Botany*, *46*, 13–28.